

Semiclassical Quantization by Harmonic Inversion: Comparison of Algorithms

Thomas Bartsch, Jörg Main, and Günter Wunner

Institut für Theoretische Physik 1, Universität Stuttgart, D-70550 Stuttgart, Germany

(November 6, 2018)

Harmonic inversion techniques have been shown to be a powerful tool for the semiclassical quantization and analysis of quantum spectra of both classically integrable and chaotic dynamical systems. Various computational procedures have been proposed for this purpose. Our aim is to find out which method is numerically most efficient. To this end, we summarize and discuss the different techniques and compare their accuracies by way of two example systems.

PACS numbers: 05.45.-a, 03.65.Sq, 02.70.-c

I. INTRODUCTION

Semiclassical trace formulae relate the spectra of quantum systems to the periodic orbits of the pertinent classical systems [1]. They yield expansions of the quantum response function of the form

$$g(E) = \sum_k \frac{d_k}{E - E_k + i\epsilon} = \sum_{\text{po}} \mathcal{A}_{\text{po}} e^{iS_{\text{po}}/\hbar}. \quad (1)$$

Here, E_k are the energy eigenvalues of the quantum system, d_k their multiplicities, S_{po} is the action of a classical periodic orbit, \mathcal{A}_{po} an amplitude that can be calculated from classical mechanics (including phase information given by the Maslov index), and the sum on the right-hand side extends over all periodic orbits and usually diverges for real energies E . Thus, the quantal information cannot be extracted directly from the semiclassical expansion.

One particular and widely applicable method to overcome the convergence problems of the periodic orbit sum is semiclassical quantization by harmonic inversion [2–4]. By a Fourier transform of Eq. (1) the problem of semiclassical quantization can be recast as a harmonic inversion problem, viz. the extraction of the frequencies $\omega_k = E_k/\hbar$ and amplitudes d_k from a given time signal

$$C(t) = \sum_k d_k e^{-i\omega_k t}. \quad (2)$$

Especially intriguing, and important, are systems possessing a classical scaling property, i.e., the classical dynamics does not depend on an external scaling parameter w and the action $S_{\text{po}} = ws_{\text{po}}$ of periodic orbits varies linearly with w , with s_{po} the scaled action. This is not a severe restriction since it covers a variety of systems, such as systems with homogeneous potentials, billiard systems, or the hydrogen atom in static external fields.

For scaling systems the semiclassical signal which has to be harmonically inverted has the special form of a sum of δ functions with peaks at positions given by the scaled actions s_{po} of the periodic orbits,

$$C(s) = \sum_{\text{po}} \mathcal{A}_{\text{po}} \delta(s - s_{\text{po}}). \quad (3)$$

The frequencies of the signal (3) are the semiclassical approximations to the quantum eigenvalues w_k of the scaling parameter. By the same token, harmonic inversion of signals with the functional form (3) also plays a key rôle in the high resolution analysis of the density of states $\varrho(E) = \sum_n \delta(E - E_n)$ of quantum spectra, in an effort to extract information about the underlying classical dynamics [4–6].

Various computational procedures have been proposed for the harmonic inversion of signals of the type (3). However, a systematic study of the relative merits and demerits of the methods and a quantitative study of their efficiencies is still lacking. To remedy this situation, we summarize and discuss different techniques of harmonic inversion and compare their accuracies in the application to two simple albeit typical example systems for which exact trace formulae are known. The aim is to pin down the numerically most efficient method for harmonic inversion.

II. HARMONIC INVERSION OF DELTA FUNCTION SIGNALS

In practical applications, the signal (3) is always known in a finite range $0 \leq s \leq S_{\text{max}}$ only. Therefore the analysis of the signal by conventional Fourier transform is limited by the “uncertainty principle”, which states that in a signal of finite length S_{max} two frequencies can only be resolved if their difference is larger than $2\pi/S_{\text{max}}$. The uncertainty principle can be circumvented by the application of high-resolution methods [7–9] which extract a discrete set of frequencies and amplitudes without imposing any *a priori* restrictions on the frequencies ω_k . However, an uncertainty remains in the weaker form of the “informational uncertainty principle” [9], which states that the signal length S_{max} required to resolve the frequencies is given by

$$S_{\text{max}} \gtrsim 4\pi\bar{\varrho}(\omega) \quad (4)$$

in terms of the local average density of frequencies $\bar{\varrho}(\omega)$. Since this relation involves the average instead of the

minimum spacing between frequencies, the signals can usually be significantly shorter than required by the Fourier transform.

Harmonic inversion of the signal (3) is a nontrivial task for the following two reasons. Firstly, the number of frequencies contained in the signal is usually large, which implies that simple methods for solving the harmonic inversion problem may be numerically unstable. Secondly, the special functional form of a signal as a sum of δ functions does not fulfill the prerequisites of several established algorithms that $C(s)$ should be known on an equidistant grid, $s = n\tau$, with $n = 0, 1, 2, \dots$ [9–11]. We briefly review the four numerical methods which so far have been successfully applied to the harmonic inversion of signals $C(s)$ given as a sum of δ functions.

Method 1 — A powerful tool for the harmonic inversion of signals given on an equidistant grid is the filter-diagonalization (FD) method of Wall and Neuhauser [7] in the version of Mandelshtam and Taylor [8,9]. The basic idea is to introduce a set of basis functions localized in frequency space and to recast the harmonic inversion problem as a generalized eigenvalue problem. For a suitable choice of the frequency window the subset of frequencies located in that window can be obtained by solving a generalized eigenvalue equation with small matrices.

To evaluate the signal (3) on an equidistant grid, the δ functions must be given an artificial width σ which spans several grid points, i.e., $\sigma > \tau$. This regularization can be achieved by convoluting the signal with a narrow, e.g., Gaussian function. In this form the FD method has been applied in Refs. [3,4] as a tool for semiclassical periodic orbit quantization.

The convolution of the signal $C(s)$ results in a damping of the amplitudes $d_k \rightarrow d_k^{(\sigma)} = d_k \exp(-w_k^2 \sigma^2/2)$. The width σ of the Gaussian function should be chosen sufficiently small to avoid an overly strong damping, e.g., by setting $\sigma \lesssim |w_{\max}|^{-1}$ where w_{\max} is the largest frequency of interest. To properly sample each Gaussian a dense grid with sufficiently small step size ($\tau \approx \sigma/3$) is required. Therefore, the convoluted signal to be processed by FD usually consists of a large number of data points, in particular when high frequency regions of the signal are to be analyzed. The numerical treatment of such large data sets may suffer from rounding errors and loss of accuracy.

Method 2 — The artificial smoothing of the signal can be circumvented when following a different approach suggested by Grémaud and Delande [6]. In contrast to Ref. [9] where the signal is assumed to be known on an equidistant grid, Grémaud and Delande start from a continuous-time formulation of the FD algorithm close to the original ansatz in [7]. Integrals involving the δ function signal (3) can then easily be calculated and expressed in terms of periodic orbit sums.

Method 3 — An alternative method to FD for high-resolution signal processing is decimated signal diag-

onalization (DSD), which was introduced by Belkić *et al.* [10,11]. DSD is a two-step process for harmonic inversion. In the first step a low-resolution frequency filter is applied by subjecting the signal to a discrete Fourier transform, selecting the Fourier components in the frequency interval of interest, and applying an inverse Fourier transform to them. The resulting band-limited signal contains only a small number of frequencies in the chosen interval and can therefore be further processed, in the second step, by conventional high-resolution methods. In this processing stage, DSD effectively uses the operational part of the discrete version of FD [9], which constructs small matrices of a generalized eigenvalue problem directly from digitized points of the band-limited decimated signal. The DSD technique is designed for signals given on an equidistant grid but can be applied to the δ function signal (3) after convolution with a narrow, e.g., Gaussian function in the same way as explained above (see Method 1).

The DSD method of Refs. [10,11] is easy to implement as it basically resorts to standard algorithms for discrete Fourier transform and matrix diagonalization. However, the application of the low-resolution Fourier filter in the first step of the method implicitly assumes periodicity of the signal (with period equal to the signal length), which is, of course, not the case in general. Therefore, DSD must be expected to be less accurate than FD (Method 1) for frequencies close to the borders of the window, or when very short frequency windows are chosen (see the discussion in Sec. III).

Method 4 — The DSD technique (Method 3) can be modified for a more direct application to the δ function signal (3) without the necessity of convoluting the signal with a narrow, e.g., Gaussian function. Because the signal $C(s)$ is given as a periodic orbit sum of δ functions the ‘filtering’ step can be performed analytically by replacing the discrete Fourier transform of Method 3 with the continuous form of the Fourier transform and expressing the integrals in terms of periodic orbit sums. This technique was proposed in Ref. [12]. The application of the analytical filter for a rectangular frequency window $[w_0 - \Delta w, w_0 + \Delta w]$ results in a band-limited (bl) signal [12]

$$C_{\text{bl}}(s) = \sum_{\text{po}} \mathcal{A}_{\text{po}} \frac{\sin[(s - s_{\text{po}})\Delta w]}{\pi(s - s_{\text{po}})} e^{is_{\text{po}}w_0}, \quad (5)$$

where the δ functions are basically replaced with sinc functions [$\text{sinc } x = (\sin x)/x$]. The band-limited signal (5) can be discretized with a small number of points and further processed, in the second step, by conventional harmonic inversion methods as described above (see Method 3).

In practice, the band-limited signal can only be evaluated approximately because the signal is only known up to a finite length. Since the sinc functions decay slowly at infinity, peaks well beyond the end of the known signal may have an influence on the band-limited signal points. Omitting contributions from the (unknown) peaks be-

yond the limit of the given signal amounts to the assumption that the signal be zero outside the given range. Note that this filter differs from the low-resolution filter of Method 3 where the signal is implicitly assumed to be periodic.

In summary, the four methods can be classified according to whether they are discrete-time algorithms (Methods 1 and 3), which require a regularization of δ function signals to be discretized, or continuous-time algorithms adapted to δ function signals (Methods 2 and 4). Alternatively, they can be classified into filter-diagonalization (FD) methods (Methods 1 and 2) and decimated signal diagonalization (DSD) methods (Methods 3 and 4) where the low-resolution ‘filtering’ and high-resolution signal processing is performed in two separate steps.

III. NUMERICAL EXAMPLES AND DISCUSSION

To quantitatively assess the relative performances of the different algorithms, we present a comparison of the numerical accuracy achieved by all of these methods for two simple but archetypal examples, viz. firstly, the high-resolution analysis of the spectrum of the harmonic oscillator and, secondly, the search for the zeros of Riemann’s zeta function as a mathematical model for periodic orbit quantization in chaotic systems. We choose these systems because they possess exact trace formulae, so that the decomposition of the semiclassical signal in a sum of exponentials is known to be exact.

A. Harmonic oscillator

The one-dimensional harmonic oscillator (with $\hbar\omega = 1$) has energy eigenvalues $E_n = n + \frac{1}{2}$, $n = 0, 1, 2, \dots$. Its density of states can be written as an exact trace formula [13]:

$$g(E) = \sum_{n=0}^{\infty} \delta(E - E_n) = \sum_{k=-\infty}^{\infty} (-1)^k e^{2\pi i k E}. \quad (6)$$

The right-hand side of Eq. (6) can be interpreted as a periodic orbit sum [in analogy to Eq. (1)] where $S_k = 2\pi k E$ is the action of the (k times traversed) periodic orbit and $d_k = (-1)^k$ is the periodic orbit amplitude. [The interpretation of the $k = 0$ Thomas-Fermi term is special, see Ref. [13] for more details.] The high-resolution analysis of the quantum spectrum $g(E) = \sum_{n=0}^{\infty} \delta(E - E_n)$ should yield equally spaced real frequencies $\omega_k = 2\pi k$ and amplitudes $d_k = (-1)^k$ of equal magnitude. Thus, this simple application of harmonic inversion to the extraction of classical periodic orbit parameters from a quantum spectrum [4–6] is ideally suited to compare the efficiencies of the different methods for the harmonic inversion of δ function signals.

Since the signal is periodic with period $\Delta E = 1$, an integer signal length would render the low-resolution Fourier filter of Method 3 exact. To avoid this atypical situation, we choose signal lengths as rational multiples of π . According to the informational uncertainty principle (4) a signal length of $E_{\max} \gtrsim 2$ should suffice to resolve the frequencies. Typically, Eq. (4) slightly underestimates the required signal length. We therefore present results calculated with a signal of length $E_{\max} = \pi$, which means that only three energy levels contribute to the signal. To assess the accuracy of the results, we use the absolute values of the imaginary parts of the calculated frequencies and amplitudes as error indicators. If the analysis of the signal were exact, all imaginary parts should vanish. Therefore, an inspection of the sizes of the imaginary parts allows us to check the accuracy of the calculation. We note that this sort of accuracy test can be applied to all bound systems. If the exact frequencies are known, as is the case in our example systems, the real parts can also be compared. The errors of the real and imaginary parts typically are of the same order of magnitude and exhibit, at least qualitatively, the same behavior.

Results for the harmonic inversion of the quantum spectrum $g(E)$ obtained with the four methods introduced in Sec. II are presented in Figs. 1 and 2 for the imaginary parts of the frequencies ω_k and amplitudes d_k , respectively. For frequencies which appear to be missing, imaginary parts of zero have been obtained by the pertinent method. From figure parts (a) to (f) the width $\Delta\omega$ of the frequency filter is increased. For the application of Methods 1 and 3 the signal has been discretized with step width $\tau = 0.002$ after convolution of the signal with a Gaussian function with width $\sigma = 0.006$. In all cases it can be seen that the precision achieved decreases to the boundaries of the frequency window. The reason is that none of the filtering methods is exact and can neither completely remove the influence of frequencies outside the window of interest nor exactly preserve the contributions of frequencies inside the window. For narrow windows, the FD methods 1 and 2 outperform the DSD algorithms 3 and 4, for wide windows the situation is reversed. The frequencies obtained by Methods 1 and 2 are equally precise for small windows, whereas for wide windows Method 2 gains superiority and even competes with the DSD methods. In general, the distance from the window boundaries where a method acquires its full precision is smaller for the FD than for the DSD methods. Calculations were carried out with double precision. For the widest window shown, frequencies have practically been obtained to machine precision.

For all methods, the precision of the amplitudes in Fig. 2 is somewhat lower than that of the frequencies in Fig. 1 because calculation of the amplitudes is done as a second step after solving the eigenvalue problem yielding the frequencies. In particular, the difference in precision between the frequencies and amplitudes is considerably

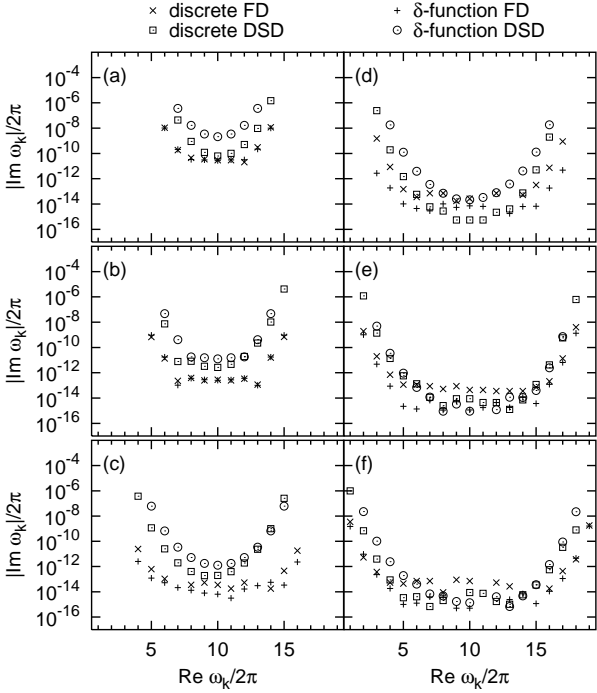


FIG. 1. Imaginary parts (absolute values) of the frequencies ω_k extracted from a harmonic oscillator signal of length $E_{\max} = \pi$. Symbols \times , $+$, \square , and \circ denote to Methods 1 to 4, respectively. Windows are $[10 - \Delta\omega, 10 + \Delta\omega]$ with $\Delta\omega =$ (a) 4.5, (b) 5.5, (c) 6.5, (d) 7.5, (e) 8.5, (f) 9.5.

larger for Method 1 than for any other method, so that even for small windows the amplitudes obtained by this technique are the least accurate (see the \times symbols in Fig. 2).

B. Zeros of Riemann's zeta function

It is a peculiar feature of the harmonic oscillator signal that the density of frequencies is constant, i.e., the precision of frequencies obtained from a signal of a given length is the same throughout the whole frequency domain. However, in typical systems the density of states grows rapidly with the frequency, which means that a longer signal is required to extract higher frequencies. As an example of a system exhibiting this typical behavior, we discuss the Riemann zeta function which has served as a mathematical model for periodic orbit quantization [3,14]. It is well known that, if the zeros of $\zeta(z)$ on the critical line $\text{Re } z = \frac{1}{2}$ are written as $z = \frac{1}{2} - iw$, the density of zeros on the critical line can be expressed as [14]

$$g(w) = -\frac{1}{\pi} \sum_p \sum_{m=1}^{\infty} \frac{\ln p}{p^{m/2}} \cos(wm \ln p), \quad (7)$$

where p runs over all prime numbers. Eq. (7) is formally identical to a semiclassical trace formula with

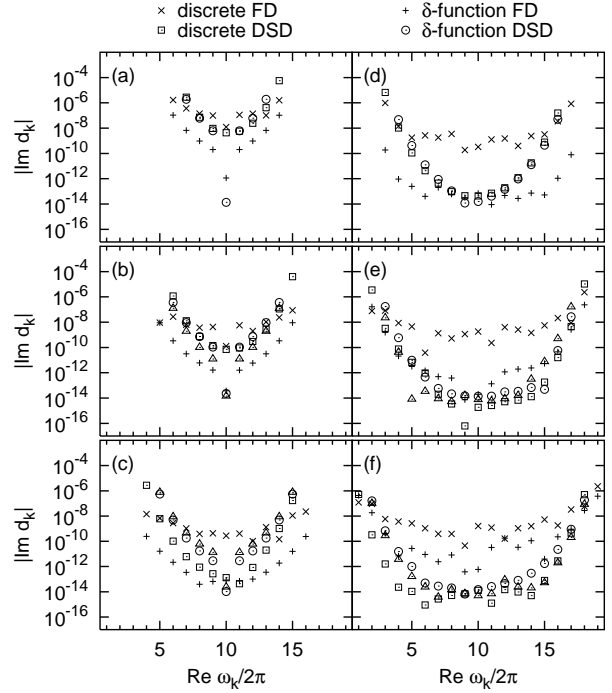


FIG. 2. Same as Fig. 1 but for the imaginary parts of the amplitudes d_k .

$S_{pm} = w m \ln p$ corresponding to classical actions and $\mathcal{A}_{pm} = (\ln p)/p^{m/2}$ corresponding to classical amplitudes. With this interpretation, the Riemann zeta function can be used as a mathematical model for chaotic dynamical systems, and the Riemann zeros are obtained by harmonic inversion of the δ function signal [3]

$$C(s) = \sum_p \sum_{m=1}^{\infty} \frac{\ln p}{p^{m/2}} \delta(s - m \ln p). \quad (8)$$

Unlike typical semiclassical trace formulae, Eq. (7) is exact. As the zeta function has only simple zeros, the amplitudes d_k obtained from the harmonic inversion of the signal (8) must all be equal to 1.

In Fig. 3 we present our numerical results obtained by application of Methods 1 to 4 to extract the (numerically complex valued) Riemann zeros with $\text{Re } w_k < 100$. Ideally, all values w_k should be real. Therefore, the absolute values of the imaginary parts of the w_k can again serve as a measure for the accuracy of the harmonic inversion process. For the application of Methods 1 and 3 the signal has been discretized with step width $\tau = 0.002$ after convolution of the signal with a Gaussian function with width $\sigma = 0.006$.

It is no problem to construct the signal (8) for the Riemann zeros up to quite large maximum values S_{\max} because only prime numbers are used as input. However, the periodic orbit quantization of physical systems usually requires a numerical periodic orbit search which becomes more and more expensive for longer orbits, especially in chaotic systems, where the number of orbits

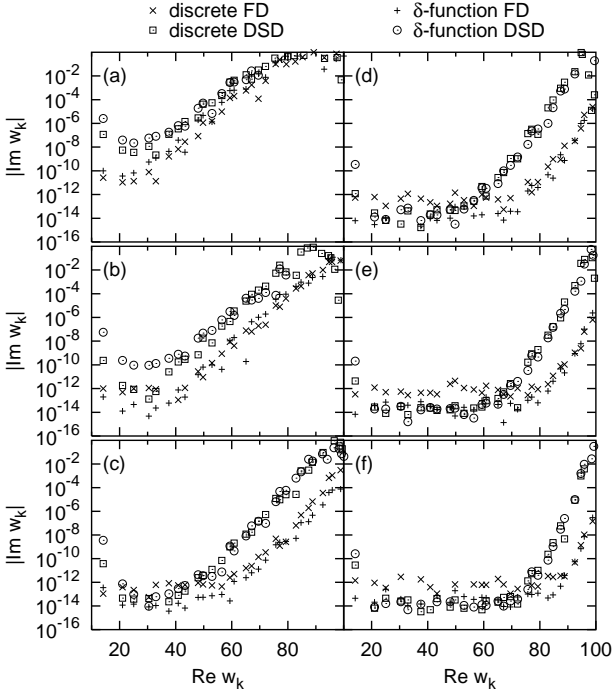


FIG. 3. Imaginary parts (absolute values) of locations w_k of zeros of the Riemann zeta function in the frequency window $[10, 100]$. Symbols \times , $+$, \square , and \circ denote to Methods 1 to 4, respectively. Signal lengths are S_{\max} = (a) 4.5, (b) 5.0, (c) 5.5, (d) 6.0, (e) 6.5, (f) 7.0.

proliferates exponentially with increasing signal length. Therefore, in practical periodic orbit quantizations the given signal length is often rather short. In Fig. 3 we present the results for the accuracy of the methods for harmonic inversion for various signal lengths, increasing from $S_{\max} = 4.5$ in Fig. 3a to $S_{\max} = 7.0$ in Fig. 3f. The frequency window $w \in [10, 100]$ is kept fixed.

For a fixed signal length, the zeros up to a certain critical value can be obtained to a constant precision. Above the critical frequency, the precision decreases rapidly due to the higher density of states. As was to be expected, for all methods the critical frequency increases with growing signal length, which means that frequencies in regions of higher spectral density can be resolved. Roughly, the critical frequency is determined by the informational uncertainty principle (4). In fact, it is slightly higher for the FD methods 1 and 2 than for the DSD methods 3 and 4. As before, the maximum accuracy below the critical frequency is obtained by the DSD methods. However, above the critical frequency the precision yielded by the FD methods is higher.

The lowest zero of the zeta function is located at $w = 14.1347$, not far above the lower boundary of the frequency window at $w = 10$. For the first zeros a decrease in accuracy due to the proximity of the boundary can be seen. Evidently, the influence of the boundary diminishes with increasing signal length. Again, it is considerably more pronounced for the DSD than for the FD methods.

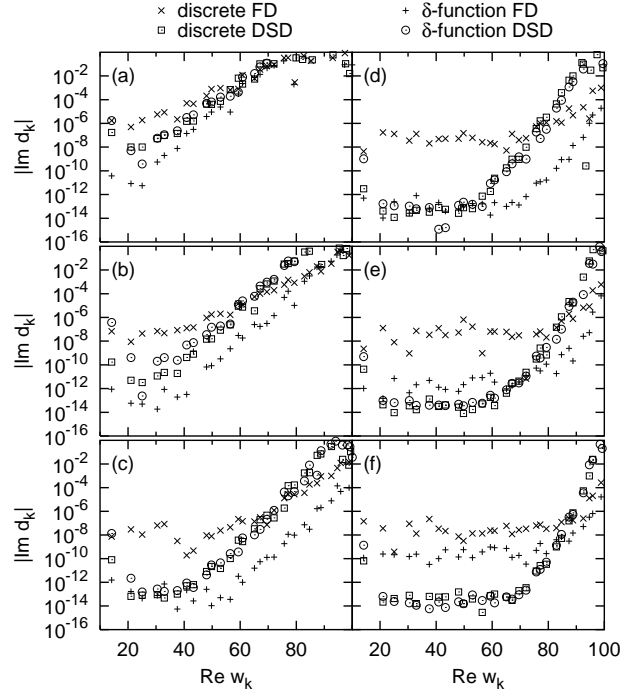


FIG. 4. Same as Fig. 3 but for the imaginary parts of the multiplicities d_k .

For the latter, it can only be seen in the shortest signals. With any of the four methods, the boundary effects on the lowest zeros can be removed if the lower boundary of the frequency window is decreased to $w = 0$.

Fig. 4 presents results similar to those shown in Fig. 3, but for the imaginary parts of the multiplicities d_k . The accuracy of the results achieved with the different methods resemble those obtained for the imaginary parts of the frequencies w_k , with the exception of Method 1 (see the \times symbols) which provides amplitudes with significantly lower precision.

IV. CONCLUSION

In this paper we have quantitatively determined the accuracies of four different algorithms for the high-resolution harmonic inversion of δ function signals, by applying all algorithms to two, physically motivated, example signals. For sufficiently long signals and broad frequency windows the four methods provide excellent results of very high accuracy, in the case of the examples selected even close to machine precision. However, when either the width of the frequency filter or the signal length is considerably reduced, the accuracy of the results obtained by the four methods can vary by several orders of magnitude.

Our calculations show that no general clear-cut answer to the question “Which method is best in all physical situations?” is possible. In practice, the window width can

be regarded as a free parameter, i.e., it can usually be chosen sufficiently large to achieve good results before increasing computational effort or numerical instabilities become a restriction. The signal length, on the contrary, is often fixed or at least hard to increase, e.g., for periodic orbit quantization of classically chaotic systems where the number of periodic orbits proliferate exponentially with the signal length. In such a case the choice of the algorithm for harmonic inversion of the signal will be essential to achieve the optimum results. When the signal length is quite at the limit for convergence of the frequencies and amplitudes, the filter-diagonalization (FD) methods 1 and 2 provide superior accuracy compared to the decimated signal diagonalization (DSD) methods 3 and 4. For signals given as the sum of δ functions Method 2 will often prove to be the method of choice.

We conclude by noting that harmonic inversion techniques can be generalized so as to cope with the analysis also of multidimensional signals, with important applications in other areas of physics [15]. The knowledge gained from the comparison of methods for one-dimensional harmonic inversion in this paper should also serve as a useful guide in future developments and applications of accurate and efficient algorithms for multidimensional high-resolution signal processing.

ACKNOWLEDGMENTS

We thank P. A. Dando and H. S. Taylor for fruitful discussions. This work was supported by the Deutsche Forschungsgemeinschaft and Deutscher Akademischer Austauschdienst.

- [10] Dž. Belkić, P. A. Dando, J. Main, H. S. Taylor, and S. K. Shin, *J. Phys. Chem. A* **104**, 11677 (2000); **105**, 514 (2001) (erratum).
- [11] Dž. Belkić, P. A. Dando, J. Main, and H. S. Taylor, *J. Chem. Phys.* **113**, 6542 (2000).
- [12] J. Main, P. A. Dando, Dž. Belkić, and H. S. Taylor, *J. Phys. A* **33**, 1247 (2000).
- [13] M. Brack and R. K. Bhaduri, *Semiclassical Physics* (Addison-Wesley, Reading, MA, 1997), chapter 3.
- [14] M. V. Berry, *Riemann's zeta function: A model for quantum chaos?* in *Quantum Chaos and Statistical Nuclear Physics*, edited by T. H. Seligman and H. Nishioka (*Lecture Notes in Physics* **263**) (Springer, Berlin, 1986), p. 1
- [15] V. A. Mandelshtam and H. S. Taylor, *J. Chem. Phys.* **108**, 9970 (1998); V. A. Mandelshtam, *J. Magn. Reson.* **144**, 343 (2000).